The Acceptance and Kinetic Resolution of alpha-Methyl Substituted Aldehydes by Norcoclaurine Synthases

Rebecca Roddan[1,2], Gudrun Gygli[3], Altin Sula[2], Daniel Méndez-Sánchez[1], Jürgen Pleiss[3], John M. Ward[4], Nicholas H. Keep[2] and Helen C. Hailes[1]*

[1]Department of Chemistry, University College London, 20 Gordon Street, London, WC1H 0AJ, UK.

[2]Institute for Structural and Molecular Biology, Department of Biological Sciences, Birkbeck, University of London, Malet Street, London, WC1E 8HX, UK.

[3]Institute of Biochemistry and Technical Biochemistry, University of Stuttgart, Stuttgart, 70569, Germany

[4]Department of Biochemical Engineering, University College London, Gower Street, London, WC1E 6BT, UK.

Corresponding author: Helen C. Hailes (h.c.hailes@ucl.ac.uk)

ABSTRACT: Norcoclaurine synthase (NCS) catalyzes a stereoselective Pictet-Spengler reaction to give the key intermediate, (*S*)-norcoclaurine in benzylisoquinoline alkaloid (BIA) biosynthesis. This family of alkaloids contains many bioactive molecules including morphine and berberine. Recently, NCS has been demonstrated to accept a variety of aldehydes and some

ketones as substrates, leading to a range of chiral tetrahydroisoquinoline (THIQ) products. Here, we report the unusual acceptance of α-substituted aldehydes, in particular α-methyl substituted aldehydes, by wild-type *Thalictrum flavum* NCS (*Δ*33*Tf*NCS) to give THIQ products. Moreover, the kinetic resolution of several α-substituted aldehydes to give THIQs with two defined chiral centers in a single step with high conversions was achieved. Several dopamine analogues were also accepted as substrates and reactions were amenable to scale-up. Active site mutants of *Tf*NCS were then used which demonstrated the potential to enhance the stereoselectivities in the reaction and improve yields. Rationale for the acceptance of these substrates and improved activity with different mutants has been gained from a co-crystallized structure of *Δ*33*Tf*NCS with a non-productive mimic of a reaction intermediate bound in the active site. Finally, molecular dynamics simulations were performed to study the binding of dopamine and an α-substituted aldehyde and provided further insight into the reaction with these substrates.

KEYWORDS: biocatalysis, norcoclaurine synthase, tetrahydroisoquinoline, Pictet-Spengler, kinetic resolution.

INTRODUCTION:

Biocatalysis continues to be viewed as a highly valuable synthetic method with several advantages compared to traditional organic synthetic approaches due to the non-hazardous reagents, ambient reaction conditions, fewer toxic by-products and higher reaction stereoselectivities. Methods such as enzyme immobilisation, novel screening methods and enzyme mutagenesis are starting to overcome many of the limitations of biocatalysis such as their poor stability, low efficiency and narrow substrate scope. Enzymes are therefore becoming a more viable, sustainable option for small molecule syntheses.[1]

The *in planta* role of norcoclaurine synthase (NCS) is the Pictet-Spengler reaction between dopamine **1** and 4-hydroxyphenylacetaldehyde (4-HPAA) to give (*S*)-norcoclaurine as a single enantiomer. Norcoclaurine is the first committed intermediate to the benzylisoquinoline alkaloid (BIA) family of natural products, so the enzyme is present in many BIA-producing plants. NCS isolated from the common meadow rue, *Thalictrum flavum* (*Tf*NCS), is one of the most studied Pictet-Spenglerases.[2–5] Indeed, the X-ray crystallographic structure has been reported together with mechanistic insights, as well as NMR studies[6], and recently and it has been established to have good substrate scope.[7–9] Notably, NCSs have been shown to accept a variety of aldehydes and ketones in place of 4-HPAA to yield different C-1 substituted tetrahydroisoquinolines (THIQs) in high stereoselectivities as the (*S*)-isomer. Very recently, density functional theory calculations have also been performed to rationalize the stereoselectivity in the NCS reaction to give (*S*)-norcoclaurine.[10]

The THIQ moiety is present in many biologically active molecules which have been shown to exhibit a variety of beneficial therapeutic activities including antibacterial[11], antitumour[12], anticoagulant[13] and muscle relaxant properties.[14,15,16] The THIQ scaffold is therefore a common target in drug discovery and thus there is a strong interest in synthesising diverse analogues and single isomer products. Accessing single enantiomer THIQ products is challenging using traditional organic synthetic methods and often requires the use of expensive and toxic chiral catalysts, multistep procedures and often poor enantiomeric excesses have been reported.[17,18] NCS is proving to be a valuable biocatalytic enzyme and has already been employed in the stereoselective syntheses of THIQs such as trolline, 1,1'- disubstituted THIQs and spiro-THIQs.[19–23]

NCS has however been reported to show poor tolerance towards α-substituted aldehydes. Previously, when Ruff *et al*. explored the use of Δ29*Tf*NCS with 2-(1-napthyl)propanal and cyclic carboxaldehydes with dopamine, no Pictet-Spenglerase products were detected, which

was rationalised as being due to a lack of conformational space in the active site (Scheme 1).[8,20] The acceptance of 1-naphthalene acetaldehyde but not 2-(1-napthyl)propanal also led to the rationale that more generally α-substituted aldehydes were not well tolerated by NCS. Interestingly, Nishihachijo *et al*. and Pesnot *et al*. reported very low levels of dopamine consumption when using α-methyl substituted aldehydes isobutanal and 2-phenylpropanal with *Coptis japonica* NCS (*Cj*NCS2), indicative that an NCS catalysed reaction may have occurred but no products were isolated or characterised.[19,21]

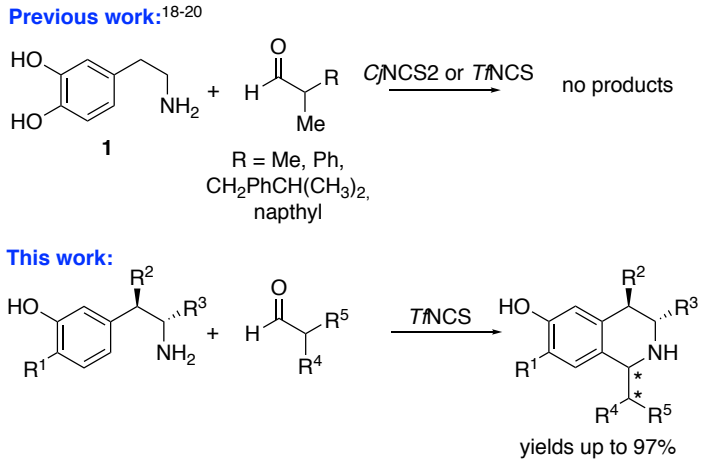

Scheme 1: NCS α-substituted aldehyde substrate scope demonstrated in previous work and in this work.

Incorporating α-methyl aldehydes into THIQs is challenging using traditional organic synthetic methods as potentially four different isomers can be formed, unless a single enantiomeric aldehyde is used, which would generate two diastereoisomers. Many single-isomer α-methyl substituted aldehydes are not commercially available and have been accessed via another available chiral molecule or synthesised using chiral auxiliary methods[24,25] and via asymmetric hydroformylation[26]. However, these methods are step-intensive, often involve the use of toxic reagents and gaining a high enantiomeric excess (e.e.) in the product is challenging. The resulting aldehyde products can also be volatile and prone to oxidation and racemisation.[27] Thus, incorporating the single enantiomer aldehyde into the product using non-enzymatic

routes is non-trivial and can lead to poor enantiopurity in the product. Accessing the resulting THIQs from reactions between a dopamine analogue and an α-methyl aldehyde is pharmaceutically relevant. Products have been reported to possess bronchodilatory activities and a corresponding isoquinoline has also been shown to have antimalarial activities.[28,29] Corydaline, a 13-methyltetrahydroprotoberberine alkaloid is also a major constituent of *Corydalis tuber* which is in clinical trials in Korea for the treatment of functional dyspepsia.[30]

Here, we report the acceptance of several α-substituted aldehydes by wild-type *Thalictrum flavum* NCS (Δ33*Tf*NCS) to give THIQ products in high yields. In addition, the kinetic resolution of α-methyl substituted aldehydes by NCS, has been achieved resulting in the formation of THIQ products with two defined stereocentres. The potential for enzyme engineering has also been explored through observing the reactions of a variety of NCS active site mutants, resulting in enhanced diastereoisomeric ratios and increased conversions. A co-crystallised structure of *Tf*NCS with a non-productive reaction intermediate analogue provided structural insights into the acceptance of these substrates. Molecular dynamics simulations of enzyme-substrate complexes were also performed to model the binding of dopamine and an α-substituted aldehyde, the (*R*)- and (*S*)-enantiomers of 2-phenylpropanal, to explore the molecular basis of stereoselectivity.

RESULTS AND DISCUSSION:

Initial NCS Reactions. Following the reported acceptance of ketones as substrates,[21] with a view to significantly extending the scope of the Pictet-Spenglerase NCS with more sterically challenging aldehydes a range of α-methyl and α-ethyl substituted aldehydes were initially tested as substrates. Reactions were investigated using wild-type NCS (WT-Δ33*Tf*NCS) and dopamine **1** with aldehydes **2a**-**7a** (Scheme 2). Remarkably, in all cases, reactions were

observed. Notably, the α-methyl substituted aldehydes **2a**-**5a** were readily accepted by *Tf*NCS to give products **2b**-**5b** in high HPLC yields (87-97%). Aldehyde **6a** was less readily accepted likely due to less rotational freedom of the alkyl chain in the active site and reduced reactivity of the conjugated aldehyde. THIQ **7b** was formed in a lower yield most likely due to steric reasons. Stereoselectivities are discussed below. Analogous reactions to the higher yielding enzyme reactions were also performed without enzyme using potassium phosphate (KPi) and acetonitrile (1:1) to give the racemic products **2b**-**5b** in 44-82% yield with no or traces of the *ortho*-product formed, reflecting the more sterically demanding nature of the α-substituted aldehydes.[31] Racemic products were generated using KPi for use as standards in chiral HPLC analyses. In all cases, reaction yields were lower in reactions using KPi as a catalyst (no NCS present) compared to with NCS, highlighting the synthetic value of the NCS-mediated reactions.

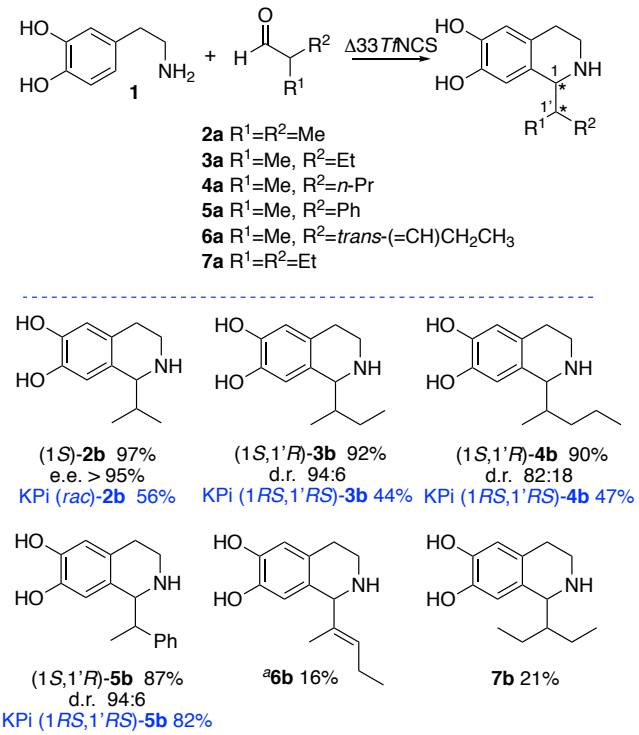

Scheme 2: *Tf*NCS reactions with **1** and the α-methyl and α-ethyl substituted aldehydes **2a**-**7a**. *Reaction conditions with NCS*: dopamine.HCl (10 mM), aldehyde (20 mM), sodium ascorbate (5 mM), Δ33*Tf*NCS (0.2 mg mL^{-1}) in HEPES buffer (100 mM, pH 7.5) with DMSO (10% *v*/*v*) at 37 °C, 250 μL scale reactions. *Reaction conditions with KPi*: dopamine.HCl (10 mM), aldehyde (20 mM), ascorbic acid (5 mM) in potassium phosphate buffer (KPi) (0.3 M, pH 6)

with acetonitrile (50% *v/v*) at 60 °C. Yields were determined by monitoring product formation against standards (by HPLC) unless otherwise indicated; Diastereoisomeric ratios (d.r.s) for stereoselective reactions were determined by ^{1}H-NMR spectroscopy; [a]The conversion was determined by monitoring dopamine consumption (HPLC, SI Section 9.2).

To extend the range of accessible THIQ products using α-methyl substituted aldehydes other amine analogues were used. Reactions were also observed with *meta*-tyramine **8**, norepinephrine **9** and metaraminol **10**. Conversions (based on amine consumption are given in Table 1) with aldehydes **2a**-**5a** were lower than those with dopamine and so product formation was confirmed by LC-MS. The lower conversions are most likely due to the different binding modes of the unnatural dopamine substrates into the active site leading to a decreased acceptance of the more challenging aldehyde substrates. However, it highlights the more general applicability of using α-methyl substituted aldehydes as NCS substrates.

Table 1: Conversions when using *α*-substituted aldehydes and a variety of different amine analogues.

Amine	Aldehyde					
	2a	**3a**	**4a**	**5a**	**6a**	**7a**
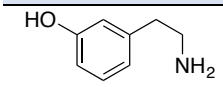 **8**	34%	48%	45%	69%	25%	26%
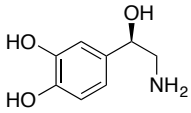 **9**	✓	65%	57%	79%	x	x
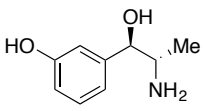 **10**	64%	50%	42%	69%	x	x

Reaction conditions: amine (10 mM), aldehyde (20 mM), sodium ascorbate (5 mM), Δ33*Tf*NCS (0.2 mg mL^{-1}) in HEPES buffer (100 mM, pH 7.5) with DMSO (10% *v/v*) at 37 °C for 18 h, 250 μL scale reactions. ✓= product observed but no conversion determined. x = no conversion observed (i.e. no product observed). Reactions were performed in triplicate and were consistent within 10% error. Conversions were determined based on amine consumption (HPLC analysis) and confirmed by the detection of the products by LC-MS data (see SI).

Reaction Stereoselectivity. For reactions with the α-methylated aldehydes, stereoselectivities were explored for the highest yielding reactions with dopamine **1**. Aldehyde **2a** is achiral: chiral HPLC analysis of **2b** indicated it was formed in >95% e.e., by comparison to the racemic standard prepared using the KPi-mediated reaction (Scheme 2), and following previous reports using *Tf*NCS this was assigned as the (*S*)-isomer.[19,32] THIQs **3b**-**5b** possess two chiral centres, and analysis of the ^{1}H NMR spectra revealed two proton environments for 1-H (*ca*. 4-5 ppm), indicating that two diastereoisomers were present. Since WT-*Tf*NCS typically generates (*S*)-THIQs at C-1, it was rationalised that the stereoselectivity at this position was retained and that a kinetic resolution of the aldehyde had occurred. Diastereoisomeric ratios (d.r.s) were determined by ^{1}H NMR spectroscopy, and high d.r.s were noted for **3b** and **5b** (94:6). To determine which aldehyde was preferentially accepted, (2*R*)-**3a** and (2*S*)-**3a** were synthesised. Aldehyde **5a** was not prepared due to the fast racemisation rates reported at pH 7.5.[33] Aldehyde (2*S*)-**3a** was synthesised from the corresponding alcohol (commercially available in 95% e.e.). The (2*R*)-isomer was prepared using an Evan's chiral auxiliary, subsequent reduction to remove the auxiliary and oxidation to give (2*R*)-**3a** (Scheme S1). For both isomers, after Swern oxidations the aldehydes were not purified by distillation or chromatographic methods to minimise the risk of racemisation: ^{1}H NMR spectroscopic data indicated reasonable levels of purity for both aldehydes, and chiral GC analysis (Figure S9) indicated (2*R*)-**3a** was formed in 79% e.e. and (2*S*)-**3a** in 68% e.e.

*Tf*NCS reactions were performed with both (2*R*)-**3a** and also (2*S*)-**3a**; yields were lower than previously, most likely due to aldehyde impurities present (see above). HPLC analysis (Scheme 3a) of the reactions under the same conditions indicated that (2*R*)-**3a** was accepted preferentially to the (2*S*)-isomer, confirming that a kinetic resolution was occurring when using the racemate. Indeed, the low levels of product formation with (2*S*)-**3a** (68% e.e.) most likely arose from the small amount of (2*R*)-isomer present (~16%). Following the established

selectivity at C-1 for *Tf*NCS and the NMR spectroscopic data, it was concluded that the major isomer formed when using racemic **3a** was (1*S*,1'*R*)-**3b** (d.r. 94:6). It was also rationalised that the same stereoselectivity arises when using **4a** to give (1*S*,1'*R*)-**4b** (d.r. 82:18) as the major isomer out of the 4 possible isomers.

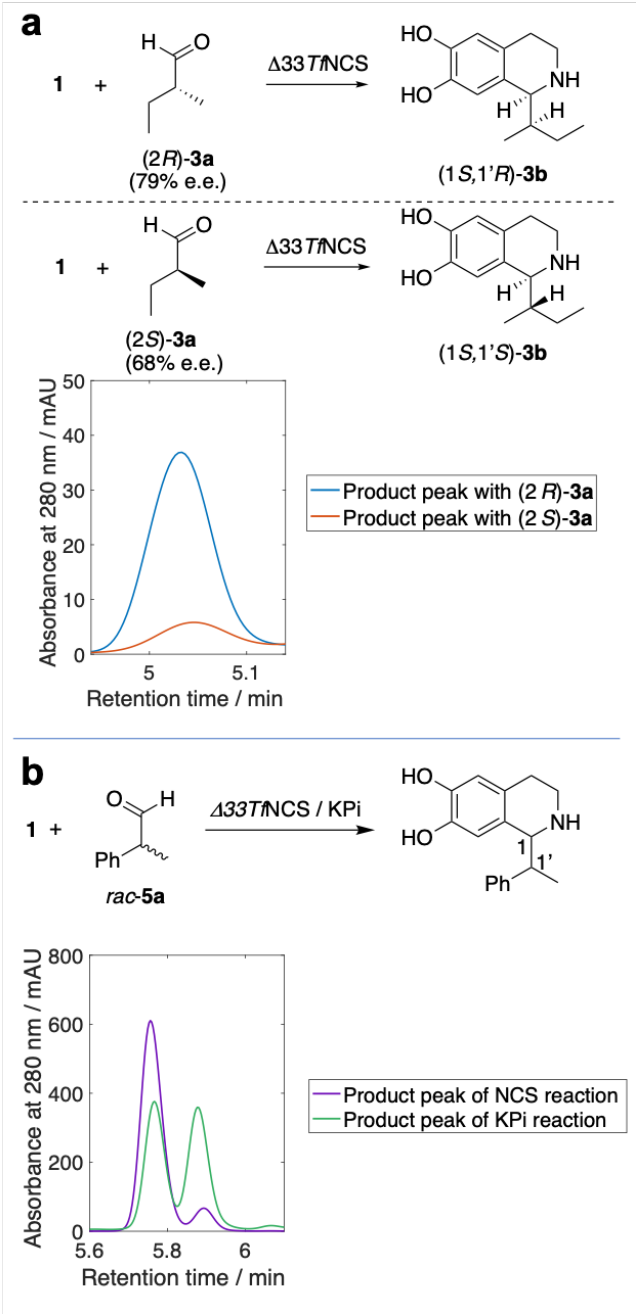

Scheme 3: a) Analytical HPLC analysis (SI Section 9.2) of enzymatic reactions between **1** and isomers (2*R*)-**3a** and (2*S*)-**3b**. *Reaction conditions:* dopamine.HCl (10 mM), (*R*)-**3a** (30 mM) or (*S*)-**3a** (30 mM) sodium ascorbate (5 mM), purified Δ33*Tf*NCS (0.2 mg mL^{-1}) in HEPES buffer (100 mM, pH 7.5) with DMSO (10% *v/v*). The total reaction volume was 250 µL and they were performed at 37 °C with results confirmed in triplicate. **b**) Analytical HPLC

analysis of enzymatic and KPi reactions between **1** and **5a**. *Reaction conditions for enzymatic reaction:* dopamine.HCl (10 mM), **5a** (20 mM), sodium ascorbate (5 mM), purified Δ33*Tf*NCS (0.2 mg mL^{-1}) in HEPES buffer (100 mM, pH 7.5) with DMSO (10% *v*/*v*) at 37 °C for 18 h, 250 μL reaction volume. *Reaction conditions for KPi reaction:* dopamine.HCl (10 mM), **5a** (20 mM), sodium ascorbate (20 mM) in KPi buffer (0.3 M, pH 6) with acetonitrile (50% *v*/*v*) at 60 °C for 18 h, 1 mL reaction volume.

HPLC analysis of **5b** generated using the non-stereoselective KPi-mediated Pictet-Spengler reaction[31], revealed two product peaks corresponding to 4-isomers (2 sets of diastereoisomers) in a ratio of 1:1 (Scheme 3b). ^{1}H NMR spectroscopy confirmed that only a trace of the *ortho*-product was formed. When compared to HPLC data for the enzymatic reaction, it was evident that an excess of one diastereoisomer was formed (ratio ~95:5) (Scheme 3b) in the enzymatic reaction which was consistent with the ^{1}H NMR data. Since arylacetaldehydes react with *Tf*NCS to give the (*S*)-isomer at C-1 in high e.e.s,[19] and following the enantioselectivity data for **3a**, this highlighted that the major product was likely to be (1*S*,1'*R*)-**5b** (d.r. 94:6). Clearly, the enzymatic reaction with WT-*Tf*NCS is an excellent route to such THIAs, as the reactions give higher yield than the KPi reaction and there is potentially stereochemical control at both chiral centres.

To determine whether the reaction could be readily scaled up, a 0.5 g scale reaction was performed using clarified cell lysate of Δ33*Tf*NCS with **1** and **3a** as the aldehyde substrate. The product was isolated via an extractive workup and the reaction went to 96% yield (HPLC yield, SI Section 9.2) and an isolated yield of 88% was achieved, consistent with the smaller scale reactions (92% HPLC yield). ^{1}H-NMR spectroscopic analysis of the product **3b** determined that the stereoselectivity of the reaction was mostly retained with a d.r. of 87:13 (small scale d.r. 94:6). The reduction in diastereoisomeric ratio is most likely due to a small amount of background phosphate-mediated reaction arising from the use of cell lysate rather than purified enzyme.

Reactions with enzyme variants. To investigate the effect of NCS variants on the acceptance of α-methyl aldehydes and products formed, several *Δ*29*Tf*NCS mutants were used as enzyme lysates, namely L76V, A79I, A79F, F80L, M97V, M97L, M97V and Y108F with **1** and **2a**, **3a**, and **5a**. Enzyme variants were chosen based upon docking experiments and previous mutagenesis studies to increase the space in the active site for bulkier substrates.[8,22] First, WT-*Δ*29*Tf*NCS was used in the reaction and no difference in reactivities or the products formed was found compared to with *Δ*33*Tf*NCS. For all three aldehydes, the mutant A79I showed higher product yields by HPLC compared to WT and the other NCS variants (Figure 1), a characteristic that has also been observed with ketones but to a greater extent.[22] This mutation has been rationalised to increase conversions of hydrophobic substrates due to enhanced hydrophobicity in the active site resulting in increased substrate affinity. For the two chiral aldehydes **3a** and **5a**, M97V showed increased yields compared to the wild-type NCS. M97 mutants have been used with ketone substrates where decreased yields were noted with a reduction in steric bulk at this position i.e. poorer conversions with M97V compared with the wild-type.[22] Interestingly, the opposite trend was observed here with aldehydes **2a** and **5a** as substrates.

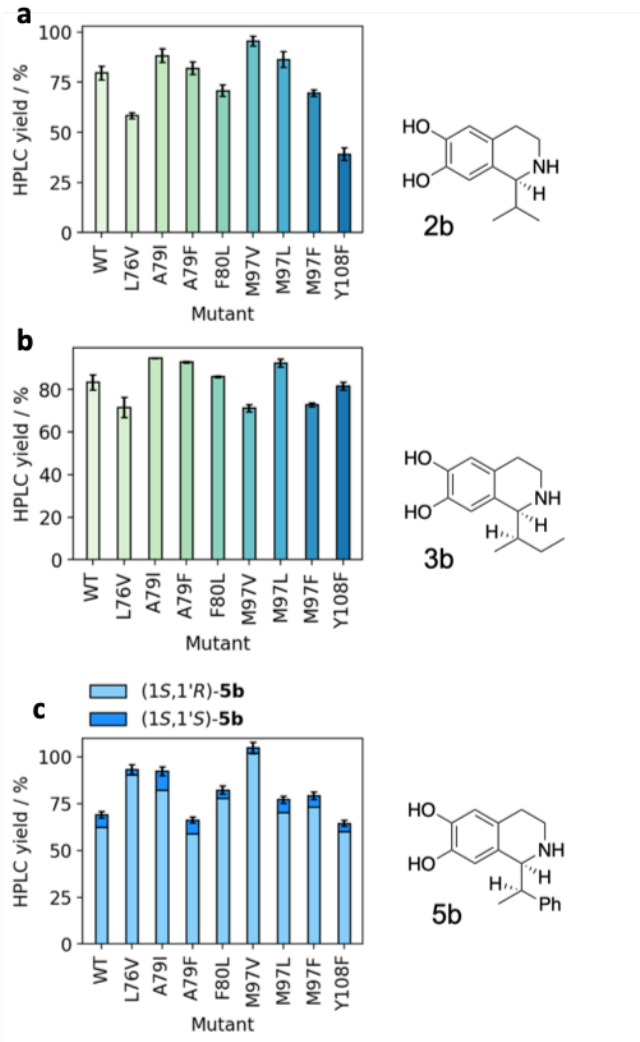

Figure 1: Yields of *Tf*NCS reactions with **1** and **2a** (**a**), **3a** (**b**) **or 5a** (**c**) to give products **2b**, **3b** and **5b** respectively. *Reaction conditions*: Dopamine.HCl (10 mM), aldehyde (20 mM), sodium ascorbate (5 mM), Δ29*Tf*NCS lysate of variant (25% *v*/*v*) in HEPES buffer (100 mM, pH 7.5) with DMSO (10% *v*/*v*) at 37 °C for 18 h, 200 µL scale reactions; Yields were determined by monitoring product formation against standards by HPLC (SI Section 9.2). Diastereoisomeric ratios of the major (1*S*,1'*R*) product to the minor (1*S*,1'*S*) product for each reaction product of **5b** are; WT, 90:10; L76V, 97:3; A79I, 89:11; A79F, 89:11; F80L, 95:5; M97V, 97:3; M97L 91:9; M97F, 92:8; Y108F, 93:7. Reactions were performed in triplicate and error bars are the standard deviations.

HPLC analysis of the reactions between **1** and **5a** showed that different active site mutants of *Tf*NCS gave different diastereoisomeric ratios of the products. A ratio of 90:10 was observed for wild-type NCS lysate, lower than with purified NCS (94:6), most likely due to the increased background phosphate reaction when using lysate. The two most promising active site mutants

observed were L76V and M97V, where product diastereoisomeric ratios of 97:3 were observed. To fully explore the change in reaction selectivity of these two mutants, both mutant enzymes (M97V and L76V) were purified and reactions performed between **1** and **2a**, **3a, 5a** and phenylacetaldehyde (**11a**). The mutant M97F was also explored to provide a comparison with the M97V mutant (Figure 2).

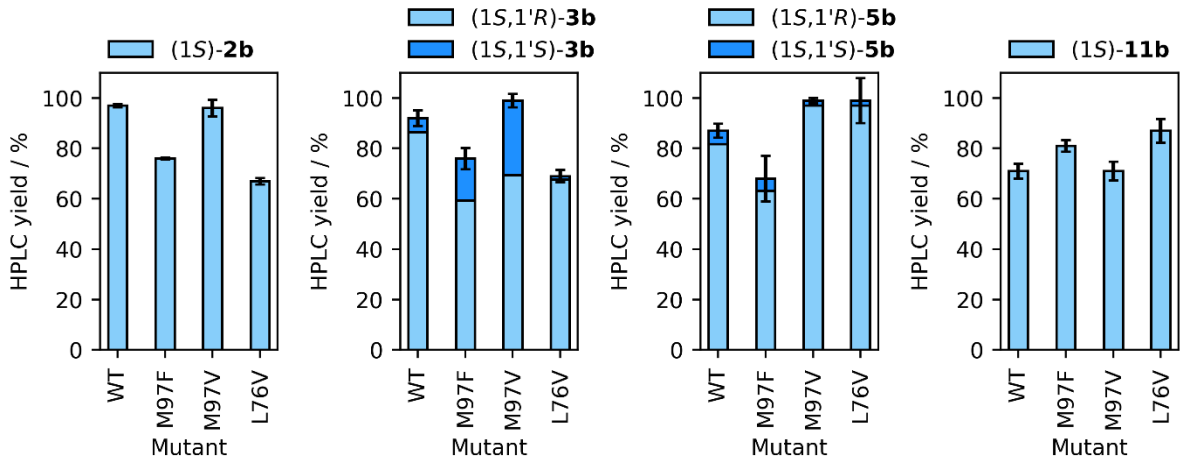

Figure 2: Yields and e.e.s of reactions of products of enzymatic reactions using purified *Tf*NCS active site mutants. *Reaction conditions:* Dopamine.HCl (10 mM), aldehyde (20 mM), sodium ascorbate (5 mM), purified *Tf*NCS (0.2 mg mL^{-1}) in HEPES buffer (100 mM, pH 7.5) with DMSO (10% *v/v*) at 37 °C for 18 h; Yields were determined by product formation against standards using HPLC (SI Section 9.2). Reactions were performed on a 250 µL scale for **2b**, **5b** and **11b**. [b]Reactions were performed on a 1 mL scale for **3b**. E.e.s were determined by chiral analytical HPLC for **2b** and **11b**. Diastereoisomeric ratios were determined by ^{1}H-NMR spectroscopy for **3b**. The diastereoisomeric ratio was determined by analytical HPLC for **5b**.

Aldehyde **11a** was used as a substrate with all three mutants to help determine whether the variants were affecting the stereochemistry of the product at the C-1 position. As previously reported, the reaction with wild-type *Tf*NCS gave a high enantiomeric excess in the product **11b**,[19] as did all the NCS variants tested here, implying that there was no effect on the stereochemistry at the C-1 position. For all reactions with **2a** as the aldehyde substrate, a high enantiomeric excess (> 95%) in the product **2b** was also retained. The enantiopurity of **2b** also demonstrated that the variants were not affecting the stereochemistry at the C-1 position of the

products with α-methyl aldehydes as substrates. Yields with M97F and L76V and **2a** as the aldehyde substrate were however slightly decreased compared to the wild-type.

Most notably, for all 3 α-methyl aldehydes tested as substrates, the products of reactions with Δ29*Tf*NCSL76V showed the same or improved stereoselectivities compared with the wild-type enzyme. There was a lowering in d.r. for all products in M97F reactions with the chiral α-methyl aldehydes, suggesting that this mutant is affecting the stereochemistry of the C-1' position. With the bulky, chiral aldehyde **5a** however, the diastereoisomeric ratio of the product **5b** was improved compared with the wild-type for both M97V and L76V mutants, and both mutants gave the product in almost quantitative yields. For both mutants, there was also little change in diastereoisomeric ratio between using purified enzyme here compared with enzymatic lysate (Figure 1), highlighting that purified enzyme is not essential for gaining a high d.r. in the product in these reactions.

Co-crystallised structure with an α-methyl reaction intermediate analogue. To rationalise the acceptance of α-methyl aldehydes by NCS, a crystal structure of *Δ*33*Tf*NCS with a non-productive mimic of a reaction intermediate bound in the active site was obtained. This was based upon previously published work in our group, wherein the 'dopamine-first' mechanism of *Tf*NCS was confirmed via a co-crystallised structure of *Δ*33*Tf*NCS with a non-productive mimic of the reaction.[9] A non-productive, secondary amine mimic (*R*)-**12** of the iminium ion intermediate of the reaction between **1** and (*R*)-**5a** was synthesised using an analogous method to the previously reported co-crystallised mimic, starting with 3,4-bis(benzoyloxy)dopamine followed by amide coupling, reduction to give the amine and subsequent deprotection to give the mimic in 14% yield. The enantiopurity of the mimic was confirmed by chiral HPLC (method 2, SI Section 9.3) as >99% e.e., using a racemic standard **12**, synthesised in an analogous manner. A single enantiomer mimic (*R*)-**12** (Scheme 4) was

used as the (*R*)-enantiomer of α-methyl aldehydes was preferentially accepted as substrates by the NCS as described above. The 'aldehyde-part' of the mimic was chosen to be (*R*)-**5a** as the phenyl group would provide extra electron density and aid identification of the ligand in the active site. Indeed, initial attempts to co-crystallise an unproductive mimic of the reaction between dopamine and racemic **3a** resulted in multiple conformations of the mimic in the active site, so the ligand could not be clearly built into the density.

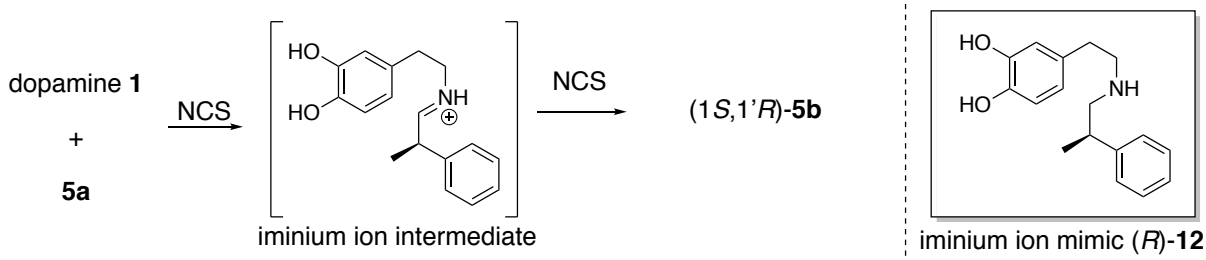

Scheme 4: Design of mimic (*R*)-**12** of the reaction between **1** and **5a**, for co-crystallisation based upon the ligand previously co-crystallised with *Δ*33*Tf*NCS (PDB: 5NON).

A co-crystallised structure of *Δ*33*Tf*NCS with mimic (*R*)-**12** in the active site was gained at 1.81 Å with a single copy in the asymmetric unit (PDB entry: 6RP3, Table S1). Compared to the previous apo structure of *Δ*33*Tf*NCS (PDB: 5N8Q), the overall fold of NCS was retained (RMSD $C_\alpha = 0.587$). The only notable difference in active side residue conformations was with Glu110 and Met97. The mimic density in the active site was less convincing than with the previously co-crystallised structure (PDB: 5NON) suggesting partial occupancy and other, minor multiple conformations of the ligand. A Polder[34] map of the ligand density showed similar density features, with some uncertainty in the placement of the dopamine ring. However, the 'aldehyde-end' of the mimic could be observed relatively clearly and so this was used to help understand why these substrates are accepted and why activity varies with single-point mutants.

In this structure (Figure 3) the ligand is placed with both hydroxyl groups of the catechol hydrogen bonded to Lys122 (with distances of 3.28 and 3.02 Å respectively) in a linear

configuration, likely reflecting a pre-cyclisation conformation. Previous studies involving the active site mutagenesis of key residues in NCS have shown that Lys122 is essential for catalytic activity.[7,8] The hydrogen bonding distances are further away than in 5NON and the mimic appears to be further buried into the active site. A hydrogen bonding interaction can also be observed between the secondary amine of the mimic and Glu110, which is in a rare conformation, observed in only 1% of glutamic acid residues in the PDB, whereas in the previous structure, the amine was bound to both Glu110 and Asp141. This interaction is consistent with the 'dopamine-first' mechanism (detailed in SI Section 4) and we are likely observing another 'snapshot' of the mechanistic process. Phe112 is present in two different conformations in the novel structure (defined at 1:1 occupancy), as in the first holo structure of *Tf*NCS (PDB: 2VQ5)[7]. In subunit B of 2VQ5, the phenylalanine conformation is uncommon, being present in only 1% of phenylalanine residues in the PDB. In structure 5NON, Phe112 is predominately in the conformation predicted by MD simulations and in subunit A of 2VQ5.[8] It is not known whether this unusual phenylalanine conformation is relevant to the NCS mechanism, perhaps suggesting an inhibitory mode with the residue acting as a 'gatekeeper', or if it is simply a crystallographic artefact.

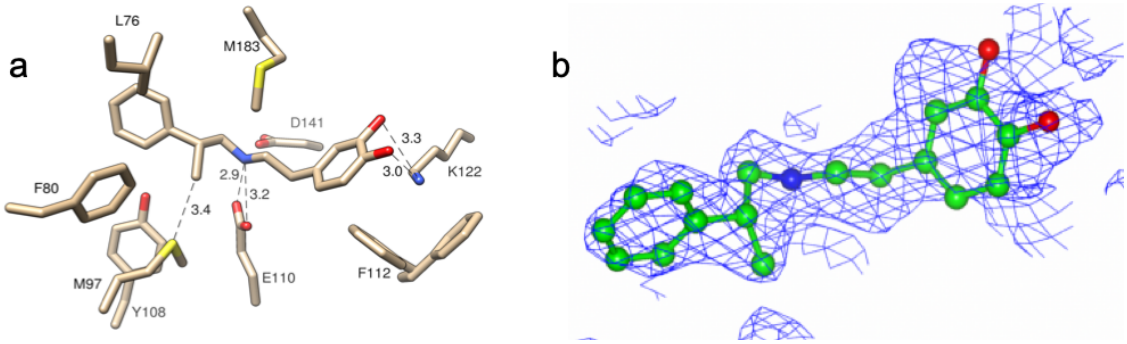

Figure 3: a) Location of mimic (*R*)-**12** in the active site. Dotted lines show key distances or hydrogen-bonding interactions. Associated numbers are distances given in Å. b) Electron density of (*R*)-**12** in the active site at contour level 0.81 RMSD.

The density of the 'dopamine-end' of the mimic was less clear so the ligand was built in with both hydroxyl groups hydrogen-bonded to Lys122, reflecting a likely mixture between the two

potential conformations, productive and inhibitory. The phenyl group of the 'aldehyde-end' of the mimic sits close to Leu76. Mutation of this residue to valine resulted in improved stereoselectivity for NCS reactions with α-methyl aldehydes. The 'aldehyde-end' of the mimic can be observed clearly and the methyl group of the mimic appears to sit close to Met97, forcing the residue into a previously unseen conformation for this residue in NCS structures. Reducing bulk at this position by mutation to a valine residue, lowers d.r.s for the reaction with aldehyde **3a**, thus providing extra space for an ethyl group and so both enantiomers of the aldehyde are more readily able to react with dopamine in the active site. However, this does not provide enough extra space for the phenyl group of **5a** and so one enantiomer is accepted preferentially. An increased d.r. in the product **5b** compared to the wild-type is likely due to improved binding of the aldehyde from this extra space provided and also leads to increased reaction yields. Conversely, the mutant M97F reduced yield and d.r.s in all products, likely due to lack of space in this region of the active site. The mutant L76V improved d.r.s with both chiral aldehydes, likely altering the shape of the active site cavity so that binding of the (*R*)-enantiomer is preferential.

Molecular dynamics simulations and mechanistic insights. With the aim of further understanding the preference for the (*R*)-enantiomer of the α-methyl aldehydes used, molecular dynamics simulations were performed. Four different starting structures with dopamine and 2-phenylpropanal bound in different positions were defined, using chain A of PDB:5NON with the ligand removed (Figure 4). In starting structures A and B, **1** was placed inside the active site, and the (*R*)- and (*S*)-enantiomers of **5a** (structures A and B, respectively) were placed at the active site entrance. In starting structures C and D, the two **5a** enantiomers were placed inside the active site ((*R*)- and (*S*)-enantiomer, respectively), and **1** at the active site entrance.

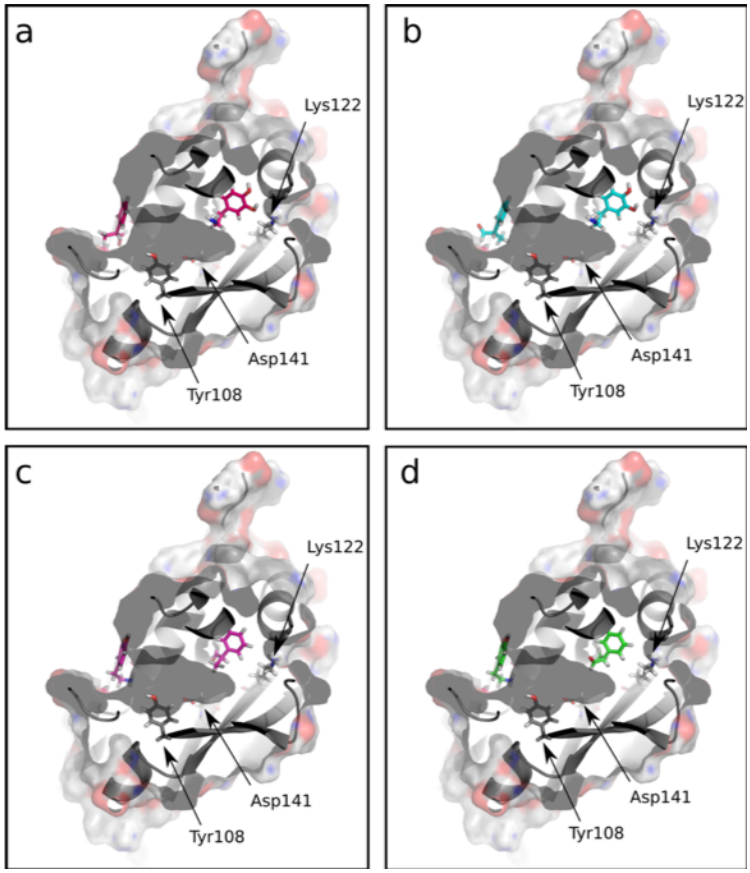

Figure 4: Four different starting structures of substrates **1** and **5a** bound to NCS. NCS is shown in as a cartoon and surface representation, allowing for identification of the active site binding pocket located as a void volume, approximately above Tyr108 and Asp141, delimited by Lys122 (right) and Tyr108 (left). Oxygen, nitrogen and hydrogen atoms are colored in red, blue and white, respectively. NCS is colored in grey and different colors of the bound substrates indicate the different starting structures. Dopamine was placed inside the active site, and the (*R*)- and (*S*)-enantiomers of **5a** (A and B, respectively) were placed at the protein surface close to the active site entrance. The aldehyde **5a** enantiomer was placed inside the active site ((*R*)- and (*S*)-enantiomer, respectively), and dopamine at the protein surface at the active site entrance (C and D, respectively). In all subsequent figures, the colors red, blue, magenta and green are used to indicate simulations starting from structures A, B, C and D, respectively.

Out of the 60 simulations launched, 58 completed successfully and two simulations with starting structure B aborted during minimisation, resulting in a total of 18.45 μs simulation time. Analyses of near attack complexes (NACs, conformers with $d_{NAC} < 4.0$ Å, see SI Section 6 for details) are summarised in Figure 5. Selected atoms of the two substrates were used for the calculation of d_{NAC} (see SI Equation 1 for details). The 1858 conformers considered to be near attack complexes amount to 0.04% of all conformers, illustrating that the productive

binding of substrates is a very rare event. Starting structure A (**1** inside the active site and (*R*)-**5a** at the protein surface) yielded most NACs with d_{NAC} < 4.0 Å (1745 conformers). Starting structures with d_{NAC} < 4.0 Å, B and C, only yielded 90 and 23 conformers, respectively. Starting structure D did not result in any conformers with d_{NAC} < 4.0 Å. The number of NACs with d_{NAC} 4.0 Å – 4.5 Å are also shown for illustrative purposes and a similar ratio of conformers across the starting structures was observed.

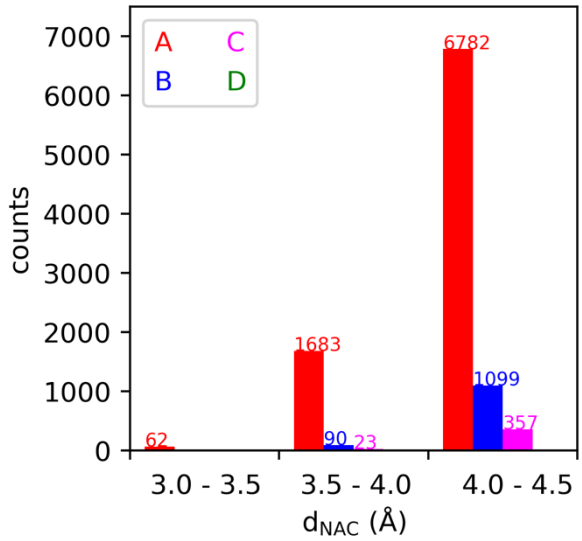

Figure 5: Near attack conformation distances below 4.5 Å for the four different starting conformations A, B, C and D (Figure 4). The number of frames with NACs between 4.0 and 4.5 Å is shown for illustration purposes.

Based on analysis of all NACs with d_{NAC} < 4.0 Å (Figure 5), it is possible to conclude that the *(R)*-enantiomer of **5a** is preferred over the *(S)*-enantiomer with a ratio 95:5 conformers (1745:90 conformers), resulting in the preferred production of the (1*S*,1'*R*)-product (**5b**). This preference agrees with the experimentally observed selectivity of NCS. Diastereoisomeric ratios (d.r.s) for these substrates were 94:6 (Scheme 2), between the (1*S*,1'*R*) and the (1*S*,1'*S*) products when racemic aldehyde was used. NAC_A therefore is most likely the NAC leading to the formation of the (1*S*,1'*R*)-product. The catalytic activity of NCS with **5a** and dopamine is rather low indicated by the need for high substrate loading (10 mM), which is in agreement

with our observation in molecular dynamics simulations, that productive substrate binding is a rare event, as only 0.04% of conformers show a NAC with $d_{NAC} < 4.0$ Å.

Visual analysis of the NACs led to the choice of representative conformers with $d_{NAC} < 4.0$ Å (Figure 6). Inspection of the substrate orientations in the active site showed that substrates showed consistent binding orientations in conformers originating from starting structure A with $d_{NAC} < 4.0$ Å (Figure 6a, NAC_A). Two different, distinct binding orientations were visible for conformers originating from starting structure B with $d_{NAC} < 4.0$ Å (Figures 6b and c, NAC_{B1}, NAC_{B2}). Another binding orientation was found for conformers originating from starting structure C with $d_{NAC} < 4.0$ Å (Figure 6d, NAC_C). Examination of the NACs showed that in NAC_A, dopamine was oriented with the amine towards the amine of Lys122, with the hydroxy groups pointing further into the active site pocket, consistent with the dopamine first mechanism. (*R*)-**5a** was located closer to Tyr108, with its phenyl ring oriented towards Tyr108 and its aldehyde group pointing towards the amine group of dopamine. Aldehyde (*R*)-**5a** was therefore located closer to the exit of the active site. For an illustration, see the movie (NACA.avi) in the SI. From analysis of the NACs with (*R*)- and (*S*)-**5a**, NAC_A was considered to be the most likely the NAC leading to the formation of the (1*S*,1'*R*)-product, so inspection of representative conformers for the other NACs will be considered briefly. NAC_{B1} was similar to NAC_A: (*S*)-**5a** was located closer to Tyr108, with its phenyl ring oriented towards Tyr108. Dopamine was located close to Ly122. In NAC_{B2}, dopamine was located below and slightly to the left of (*S*)-**5a**. The amine of dopamine pointed away from Tyr108 and the two hydroxyl groups pointed towards Asp141. In NAC_C, **1** was located close to Tyr108, with its amine group oriented towards the hydroxyl group of Tyr108. All molecules were allowed to move freely, so it was possible that both substrates unbind from NCS and interact only with each other and the solvent. This was only observed in 9 conformers with $d_{NAC} < 4.0$ Å. Root mean square function (RMSF) data showed a trend towards slightly higher RMSF values for simulations

with starting structures A and B (Figure S6). This trend was stronger when only considering NAC with d_{NAC} < 4.0 Å (Figure S7). It is unclear whether this slightly increased flexibility impacts the mechanism of NCS.

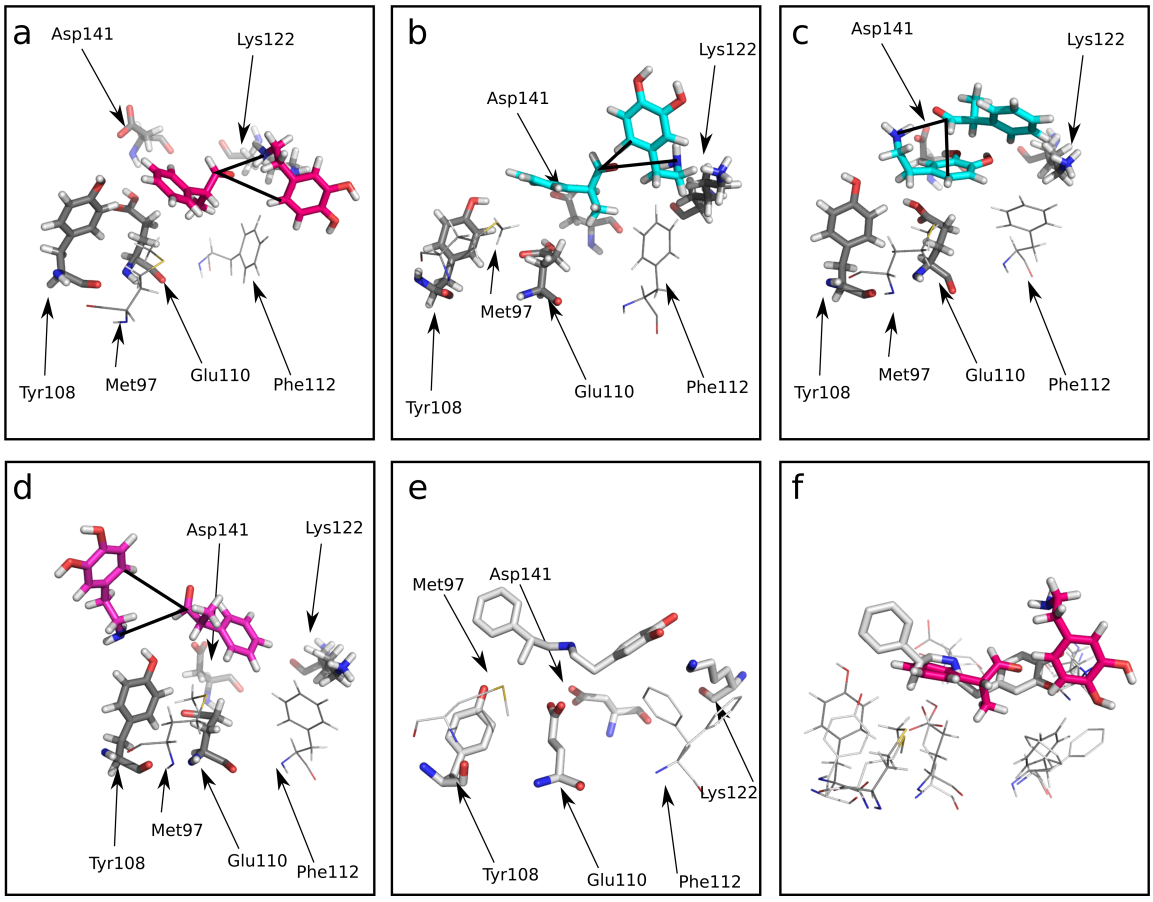

Figure 6: Figures a-d) are representative near attack complexes (NAC_A, NAC_{B1}, NAC_{B2} and NAC_C) of simulations with starting structures A, B and C. Black, thick lines indicate the distances between atoms used to calculate d_{NAC}. Figure e) shows the iminium ion mimic from PDB 6RP3 from the same viewpoint as the representative NACs. Figure f) shows NAC_A aligned with the iminium ion mimic from PDB 6RP3. Note that Figure e shows parts of a crystal structure, thus missing hydrogen atoms, and that Figure f shows the crystal structure (in white) aligned with NAC_A, which contains hydrogen atoms that were added for the simulations.

Two conflicting mechanisms have been proposed for aldehyde activation and loss of water to allow formation of the iminium ion intermediate.[8,9] Briefly, in the 'aldehyde first' mechanism, aldehyde activation is proposed to involve Lys122, with Tyr108 having a role in catechol deprotonation. However, since experimentally, bulky aldehyde substrates are

converted to THIQs, subsequent *in silico* modelling and a crystal structure with an imine intermediate analogue led to the proposed 'dopamine first' mechanism.[8,9] In this mechanism, Glu110 is suggested to play the major role (together with Asp141 and Tyr108) in aldehyde activation and imine formation, with Lys122 deprotonating the catechol.

In the reaction between **1** and (*R*)-**5a**, starting structure A where dopamine is positioned inside the active site leads to the most NACs (NAC_A). This indicates that the reaction is much more likely to happen if dopamine is bound to NCS first, followed by the aldehyde. Distances in NAC_A between substrate and the proposed catalytic residues were measured as an indicator for catalytic activity (Figure 7).

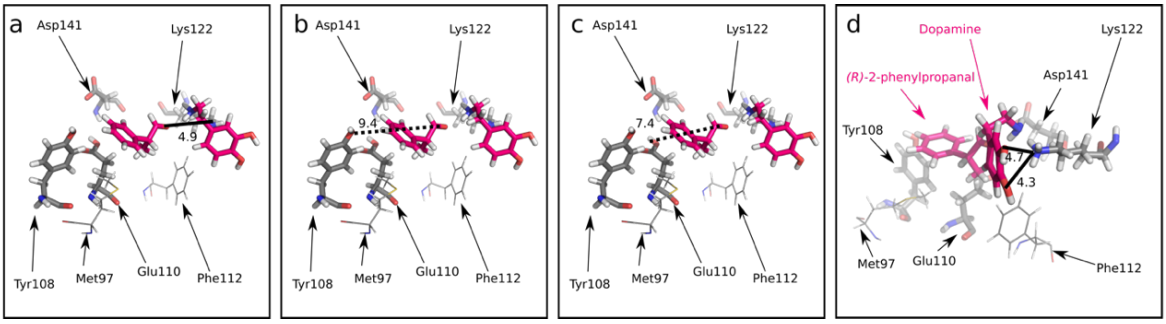

Figure 7: Distances of the aldehyde functional group to key catalytic residues in the most prevalent near attack complexes, originating from starting structure A, NAC_A. Distance from the carbon of the aldehyde functional group to the a) nitrogen on Lys122, b) phenolic oxygen of Tyr108, c) oxygen of Glu110. d) Distances from the dopamine catechol oxygens to the nitrogen of Lys122.

For NAC_A the distances between the substrate aldehyde carbon and Lys122 nitrogen and Tyr108 phenolic oxygen were 4.9 Å and 9.4 Å, respectively (Figure 7a,b). In addition, the distance between the substrate aldehyde carbon and Glu110 was 7.4 Å (Figure 7c). Assuming the dopamine first mechanism, this suggests that upon aminol formation, a movement of the substrate aldehyde towards Glu110 is required to facilitate the loss of water.[8] The orientation of the meta-hydroxyl group of dopamine is crucial for NCS activity,[7] which is supported by the observed distances between the hydroxyl groups of dopamine to the Lys122 nitrogen (4.7 Å and 4.3 Å, for meta and para hydroxyl groups respectively, Figure 7d). Distances of the

dopamine amine to Asp141 and Glu110 were too far to allow hydrogen bonding (10.1 and 9.8 Å, respectively, data not shown). Assuming the dopamine first mechanism, this suggests that upon aminol formation, a movement of the substrate dopamine towards Glu110 is required to facilitate the imine formation and cyclization. Indeed, the previous NMR study highlighted structural changes upon substrate complexation.[6] The relative orientation of the substrates to each other in NAC_A is identical to the iminium ion mimic in the crystal structure, although the position of the substrates is slightly shifted (Figures 6e,f). The observed differences could indicate that upon formation of the aminol or the iminium ion intermediates, a slightly different binding interaction in the active site arises, compared to the individual substrates. In $NAC_{B1,}$ NAC_{B2} and NAC_C the orientation and position of substrates is different to the crystal structure.

Molecular dynamics simulations were performed in a workflow, allowing repeatable simulation of the different starting structures in 15 replicates, as described in more detail in the methods section. We would like to highlight the fact that due to our workflow, we were able to conveniently perform and analyse in total 60 molecular simulations (4 starting structures, 5 replicates of 100 ns each and 10 replicates of 400 ns each). Extensive sampling by long simulations and multiple replicates is crucial for obtaining sufficient sampling of rare events like productive binding of substrates to the active site. Overall, the simulations were useful to rationalise the enantioselectivity observed and indicate initial positioning of the substrates in the active site.

In summary, this work shows that α-methyl substituted aldehydes are accepted as substrates by wild-type *Tf*NCS using both dopamine and a variety of analogues as the amine substrate. Products were generated in high yields (up to 97%) with high enantiomeric excess (>99%), or diastereoisomeric ratios (up to 94:6) with chiral α-methyl substituted aldehydes, providing a sustainable, facile route to these compounds. For chiral α-methyl substituted aldehydes the THIQ products were generated with two defined chiral centres, with (1*S*,1'*R*)-stereochemistry

as determined by the synthesis of two enantiomeric aldehydes. Active site mutants were capable of improving the diastereoisomeric ratios in the products (up to 98:2) with chiral α-methyl substituted aldehydes and improved the reaction yields with several aldehydes. The enzymatic reaction was confirmed to occur via a mechanism that involves dopamine binding first to the active site, from a co-crystallized structure of Δ33*Tf*NCS with a reaction intermediate mimic in the active site. Molecular dynamics simulations were performed to investigate the binding of dopamine and the (*R*)- and (*S*)-enantiomers of 2-phenylpropanal, into the NCS active site. The simulations provided supporting data that a kinetic resolution of the α-methyl substituted aldehyde was occurring and that the (*R*)-enantiomer of aldehyde was accepted preferentially.

Accession codes

The crystal structure reported has been deposited in the Protein Data Bank as entry 6RP3.

AUTHOR INFORMATION

Corresponding Author

*Helen. C. Hailes. Email: h.c.hailes@ucl.ac.uk

Author Contributions

The manuscript was written through contributions of all authors. R.R. performed chemical syntheses, chemical characterization, enzymatic assays and created figures. R.R. and A.S conducted protein purifications and crystallization trials. A.S. collected x-ray diffraction data which was processed and analyzed by N.K., A.S., and R.R. G.G. performed molecular dynamics simulations and their analysis and created figures. D.M.-S. expressed *Tf*NCS mutants. The project was supervised by J.M.W, N.K, J.P. and H.C.H. The manuscript was

written by H.C.H, J.P, R.R. and G.G. All authors have given approval to the final version of the manuscript.

Funding Sources

This work was funded in part by a Birkbeck PhD studentship to R.R as part of the London Interdisciplinary Doctoral Programme. Funding from the Biotechnology and Biosciences Research Council (BBSRC) to D. M.-S. (BB/N01877X/1) is gratefully acknowledged. Financial support from the Swiss National Science Foundation (SNF) of G.G. by an "Early Postdoc Mobility" fellowship is gratefully acknowledged. G.G. and J.P. acknowledge financial support by Deutsche Forschungsgemeinschaft (EXC310 and EXC2075). We also acknowledge equipment support from the Engineering and Physical Sciences Research Council (EPSRC) (EP/P020410/1).

Notes

The authors declare no competing financial interest.

ABBREVIATIONS

NCS, norcoclaurine synthase; BIA, benzylisoquinoline alkaloid; THIQ, tetrahydroisoquinoline, *Tf*, *Thalictrum flavum*; 4-HPAA, 4-hydroxyphenylacetaldehyde; NMR, nuclear magnetic resonance; e.e., enantiomeric excess; WT, wild-type; KPi, inorganic phosphate; DMSO, dimethylsulfoxide; d.r., diasteromeric ratio; HPLC, high performance liquid chromatography; LC-MS, liquid chromatography-mass spectrometry; GC, gas chromatography; MD, molecular dynamics; RMSF, root mean square function.

Supporting Information.

The supporting information is available free of charge on the ACS Publications website at DOI: xxxx. Experimental methods, supporting Figures and Tables and chemical characterization are given (PDF).

ACKNOWLEDGMENTS

We acknowledge Helena Philpott for chiral GC analysis. We also thank K. Karu (UCL Mass Spectrometry Facility) and A. E. Aliev (UCL NMR Facility) in the Department of Chemistry at UCL. Simulations were performed on the computational facility BinAC funded by the State of Baden-Württemberg, Germany, within the framework program bwHPC and the Deutsche Forschungsgemeinschaft (INST 39/963-1 FUGG).

REFERENCES

(1) Sheldon, R. A.; Woodley, J. M. Role of Biocatalysis in Sustainable Chemistry. *Chem. Rev.* **2018**, *118*, 801–838.

(2) Samanani, N.; Facchini, P. J. Purification and Characterization of Norcoclaurine Synthase The First Committed Intermediate in Benzylisoquinoline Alkaloid Biosynthesis in Plants. *J. Biol. Chem.* **2002**, *277*, 33878–33883.

(3) Luk, L. Y. P.; Bunn, S.; Liscombe, D. K.; Facchini, P. J.; Tanner, M. E. Mechanistic Studies on Norcoclaurine Synthase of Benzylisoquinoline Alkaloid Biosynthesis: An Enzymatic Pictet-Spengler Reaction. *Biochemistry* **2007**, *46*, 10153–10161.

(4) Pasquo, A.; Bonamore, A.; Franceschini, S.; Macone, A.; Boffi, A.; Ilari, A. Structural

Biology and Crystallization Communications Cloning, Expression, Crystallization and Preliminary X-Ray Data Analysis of Norcoclaurine Synthase from Thalictrum Flavum. *Cryst. Commun. Acta Cryst* **2008**, *64*, 281–283.

(5) Bonamore, A.; Rovardi, I.; Gasparrini, F.; Baiocco, P.; Barba, M.; Molinaro, C.; Botta, B.; Boffi, A.; Macone, A. An Enzymatic, Stereoselective Synthesis of (S)-Norcoclaurine. *Green Chem.* **2010**, *12*, 1623–1627.

(6) Berkner, H.; Schweimer, K.; Matecko, I.; Osch, P. Conformation, Catalytic Site, and Enzymatic Mechanism of the PR10 Allergen-Related Enzyme Norcoclaurine Synthase. *Biochem. J* **2008**, *413*, 281–290.

(7) Ilari, A.; Franceschini, S.; Bonamore, A.; Arenghi, F.; Botta, B.; Macone, A.; Pasquo, A.; Bellucci, L.; Boffi, A. Structural Basis of Enzymatic (S)-Norcoclaurine Biosynthesis. *J. Biol. Chem.* **2009**, *284*, 897–904.

(8) Lichman, B. R.; Gershater, M. C.; Lamming, E. D.; Pesnot, T.; Sula, A.; Keep, N. H.; Hailes, H. C.; Ward, J. M.; Ward, C. J. M. "Dopamine-First" Mechanism Enables the Rational Engineering of the Norcoclaurine Synthase Aldehyde Activity Profile. *FEBS J.* **2015**, *282*, 1137–1151.

(9) Lichman, B. R.; Sula, A.; Pesnot, T.; Hailes, H. C.; Ward, J. M.; Keep, N. H. Structural Evidence for the Dopamine-First Mechanism of Norcoclaurine Synthase. *Biochemistry* **2017**, *56*, 5274–5277.

(10) Sheng, X.; Himo, F. Enzymatic Pictet–Spengler Reaction: Computational Study of the Mechanism and Enantioselectivity of Norcoclaurine Synthase. *J. Am. Chem. Soc.* **2019**, *141*, 11230–11238.

(11) Iwasa, K.; Moriyasu, M.; Tachibana, Y.; Kim, H.-S.; Wataya, Y.; Wiegrebe, W.;

Bastow, K. F.; Cosentino, L. M.; Kozuka, M.; Lee, K.-H. Simple Isoquinoline and Benzylisoquinoline Alkaloids as Potential Antimicrobial, Antimalarial, Cytotoxic, and Anti-HIV Agents. *Bioorganic Med. Chem.* **2001**, *9*, 2871–2884.

(12) Ishiguro, K.; Sakiyama, S.; Takahashi, K.; Arai, T. Mode of Action of Saframycin A, a Novel Heterocyclic Quinone Antibiotic. Inhibition of RNA Synthesis in Vivo and in Vitro. *Biochemistry* **1966**, *119*, 566–3775.

(13) Al-Horani, R. A.; Mehta, A. Y.; Desai, U. R. Potent Direct Inhibitors of Factor Xa Based on the Tetrahydroisoquinoline Scaffold. *Eur. J. Med. Chem.* **2012**, *54*, 771–783.

(14) Ikeda, K.; Kobayashi, S.; Suzuki, M.; Miyata, K.; Takeuchi, M.; Yamada, T.; Honda, K. M3 Receptor Antagonism by the Novel Antimuscarinic Agent Solifenacin in Urinary Bladder and Salivary Gland. *Naunyn. Schmiedebergs. Arch. Pharmacol.* **2002**, *366*, 97–103.

(15) Hagel, J. M.; Facchini, P. J. Benzylisoquinoline Alkaloid Metabolism: A Century of Discovery and a Brave New World. *Plant Cell Physiol.* **2013**, *54*, 647–672.

(16) Yang, G.-M.; Sun, J.; Pan, Y.; Zhang, J.-L.; Xiao, M.; Zhu, M.-S. Isolation and Identification of a Tribenzylisoquinoline Alkaloid from Nelumbo Nucifera Gaertn, a Novel Potential Smooth Muscle Relaxant. *Fitoterapia* **2017**, *124*, 58–65.

(17) Werner, F.; Blank, N.; Opatz, T. Synthesis of (–)-(S)-Norlaudanosine, (+)-(R)-O,O-Dimethylcoclaurine, and (+)-(R)-Salsolidine by Alkylation of an α-Aminonitrile. *European J. Org. Chem.* **2007**, 3911–3915.

(18) Ferraccioli, R.; Giannini, C.; Molteni, G. Stereoselective Synthesis of 1,3-Substituted Tetrahydroisoquinolines through Palladium-Catalyzed Three-Component Reaction. *Tetrahedron* **2007**, *18*, 1475–1480.

(19) Pesnot, T.; Gershater, M. C.; Ward, J. M.; Hailes, H. C. The Catalytic Potential of Coptis Japonica NCS2 Revealed - Development and Utilisation of a Fluorescamine-Based Assay ETI. *Adv. Synth. Catal.* **2012**, *354*, 2997–3008.

(20) Ruff, B. M.; Bräse, S.; O'Connor, S. E. Biocatalytic Production of Tetrahydroisoquinolines. *Tetrahedron Lett.* **2012**, *53*, 1071–1074.

(21) Nishihachijo, M.; Hirai, Y.; Kawano, S.; Nishiyama, A.; Minami, H.; Katayama, T.; Yasohara, Y.; Sato, F.; Kumagai, H. Asymmetric Synthesis of Tetrahydroisoquinolines by Enzymatic Pictet-Spengler Reaction. *Biosci. Biotechnol. Biochem.* **2014**, *78*, 701–707.

(22) Lichman, B. R.; Zhao, J.; Hailes, H. C.; Ward, J. M. Enzyme Catalysed Pictet-Spengler Formation of Chiral 1,1'-Disubstituted- and Spiro-Tetrahydroisoquinolines. *Nat. Commun.* **2017**, *8*, 14883.

(23) Zhao, J.; Lichman, B. R.; Ward, J. M.; Hailes, H. C. One-Pot Chemoenzymatic Synthesis of Trolline and Tetrahydroisoquinoline Analogues. *Chem. Commun.* **2018**, *54*, 1323–1326.

(24) Evans, D. A.; Ennis, M. D.; Mathre, D. J. Asymmetric Alkylation Reactions of Chiral Imide Enolates. *J. Am. Chem. Soc.* **1982**, *104*, 1737–1739.

(25) Evans, D. A.; Bartroli, J.; Shih, T. L. Enantioselective Aldol Condensations. *J. Am. Chem. Soc.* **1981**, *103*, 2127–2129.

(26) Nozaki, K.; Sakai, N.; Nanno, T.; Higashijima, T.; Mano, S.; Horiuchi, T.; Takaya, H. Highly Enantioselective Hydroformylation of Olefins Catalysed by Rhodium(I) Complexes of New Chiral Phosphine-Phosphite Ligands. *J. Am. Chem. Soc.* **1997**, *119*, 4413–4423.

(27) Galletti, P.; Emer, E.; Gucciardo, G.; Quintavalla, A.; Pori, M.; Giacomini, D. Chemoenzymatic Synthesis of (2S)-2-Arylpropanols through a Dynamic Kinetic Resolution of 2-Arylpropanals with Alcohol Dehydrogenases. *Org. Biomol. Chem.* **2010**, *8*, 4117.

(28) Craig, P. N.; Nabenhauer, F. P. 1-Alkyl-6,7-Dihydroxyl-1,2,3,4-Tetrahydroisoquinoline Compounds. *United States Pat. Off.* **1953**, 1.

(29) Iwasa, K.; Moriyasu, M.; Tachibana, Y.; Kim, H.-S.; Wataya, Y.; Wiegrebe, W.; Bastow, K. F.; Cosentino, L. M.; Kozuka, M.; Lee, K.-H. Simple Isoquinoline and Benzylisoquinoline Alkaloids as Potential Antimicrobial, Antimalarial, Cytotoxic, and Anti-HIV Agents. *Bioorganic Med. Chem.* **2001**, *9*, 2871–2884.

(30) Lee, T. H.; Son, M.; Kim, S. Y. Effects of Corydaline from Corydalis Tuber on Gastric Motor Function in an Animal Model. *Bio. Pharm. Bull.* **2010**, *6*, 958–962.

(31) Pesnot, T.; Gershater, M. C.; Ward, J. M.; Hailes, H. C. Phosphate Mediated Biomimetic Synthesis of Tetrahydroisoquinoline Alkaloids. *Chem. Commun.* **2011**, *47*, 3242–3244.

(32) Stadler, R.; Kutchan, T. M.; Zenk, M. H. (S)-Norcoclaurine Is the Central Intermediate in Benzylisoquinoline Alkaloid Biosynthesis. *Phytochemistry* **1989**, *28*, 1083–1086.

(33) Galletti, P.; Emer, E.; Gucciardo, G.; Quintavalla, A.; Pori, M.; Giacomini, D. Chemoenzymatic Synthesis of (2S)-2-Arylpropanols through a Dynamic Kinetic Resolution of 2-Arylpropanals with Alcohol Dehydrogenases. *Org. Biomol. Chem.* **2010**, *8*, 4117–4123.

(34) Liebschner, D.; Afonine, P. V.; Moriarty, N. W.; Poon, B. K.; Sobolev, O. V.; Terwilliger, T. C.; Adams, P. D. Polder Maps: Improving OMIT Maps by Excluding Bulk Solvent. *Acta Crystallogr. Sect. D Struct. Biol.* **2017**, *73*, 148–157.

TABLE OF CONTENTS GRAPHIC: